Base-Free Oxidation of Alcohols to Esters at Room Temperature and Atmospheric Conditions using Nanoscale Co-Based Catalysts

Wei Zhong, Hongli Liu, Cuihua Bai, Shijun Liao, and Yingwei Li*

Key Laboratory of Fuel Cell Technology of Guangdong Province, School of Chemistry and Chemical Engineering, South China University of Technology, Guangzhou 510640, People's Republic of China

Ⓢ *Supporting Information*

ABSTRACT: The direct oxidation of alcohols to esters with molecular oxygen is an attractive and crucial process for the synthesis of fine chemicals. To date, the heterogeneous catalyst systems that have been identified are based on noble metals or have required the addition of base additives. Here, we show that Co nanoparticles embedded in nitrogen-doped graphite catalyze the aerobic oxidation of alcohols to esters at room temperature under base-free and atmospheric conditions. Our Co@C-N catalytic system features a broad substrate scope for aromatic and aliphatic alcohols as well as diols, giving their corresponding esters in good to excellent yields. This apparently environmentally benign process provides a new strategy with which to achieve selective oxidation of alcohols.

Co:
C:
N:

Yield up to >99%
34 examples
Mild conditions
Gram scale

1 atm, air
25 °C

Alcohols   Esters

KEYWORDS: alcohols, cobalt, heterogeneous catalysis, metal−organic frameworks, oxidation
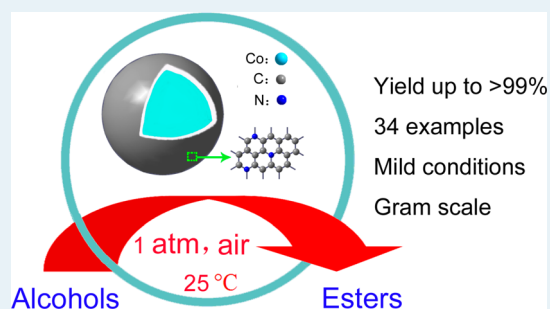
INTRODUCTION

The selective oxidation of alcohols is widely recognized as one of the most important transformations in organic synthesis because of the importance and versatility of the corresponding carbonyl products for the fine and bulk chemical industry. Among these carbonyl compounds, esters represent an abundant class of chemicals, widely utilized in fine chemicals, natural products, pharmaceuticals, agrochemicals, and food additives.[1] Traditionally, esters are prepared by the reaction of carboxylic acids or activated acid derivatives (acyl chlorides and anhydrides) with alcohols, a multistep process often accompanied by the formation of large amounts of undesired byproducts.[2] In recent years, a great deal of research effort has been devoted to the development of environmentally benign and cost-effective procedures for the synthesis of esters as alternatives for traditional protocols: e.g., the catalytic esterification of aldehydes with alcohols.[3] Of the well-established methodologies, the oxidative direct esterification of alcohols with molecular oxygen may be the most preferred and promising,[4] which could represent a big step forward toward green, economic, and sustainable processes because of the availability and low cost of alcohols in comparison to their oxidation products such as aldehydes and acids.

Many catalytic systems, including both homogeneous and heterogeneous catalysts, have been developed for the oxidation of alcohols to esters. From an economic and environmental viewpoint, the use of heterogeneous catalysts would be beneficial with respect to catalyst separation and recycling. Nevertheless, most of the heterogeneous catalysts for the oxidative esterification of alcohols with molecular oxygen were based on noble metals such as gold[5] and palladium.[6] Moreover,

satisfactory results were obtained in only limited cases, in which a large excess of base additives was required, and this was usually achieved at relatively high temperatures and/or high pressures. Therefore, the development of reusable catalysts (ideally based on non-noble metals) for the oxidative direct esterification of alcohols under mild conditions (preferably at room temperature under atmospheric conditions) is an attractive and challenging subject in both green chemistry and organic synthesis.

Here, we report the first example of a highly efficient and reusable cobalt-based catalyst for catalytic direct oxidation of alcohols to esters at room temperature under atmospheric conditions without the assistance of any base additives. In comparison with the already disclosed synthesis methodologies, this novel catalytic system would hold multiple advantages, including cost effectiveness (using nonprecious metals as catalyst and air as oxidant), environmental safety (at room temperature under atmospheric conditions without the addition of base additives), and simplicity (easy operation under ambient conditions and facile magnetic separation of the catalyst). Moreover, the proposed catalytic system features a broad substrate scope for aromatic and aliphatic alcohols as well as diols, providing good to excellent yields of the target products with high selectivities. These give the catalyst system great potential for industrial application in the production of esters from direct aerobic oxidation of alcohols.

The Co@C-N (carbon–nitrogen embedded cobalt nano-paticles) materials were prepared by simple thermolysis of a Co-containing metal–organic framework (MOF), ZIF-67. MOFs are an emerging class of ordered porous materials built with metal ions and organic ligands. Owing to their high surface area, porosity, and chemical tunability, MOFs have shown great potential for applications in a wide range of fields such as catalysis, luminescence, gas storage, and separation.[7] On the other hand, taking advantage of their ordered structures and relatively low thermal stability, MOFs could be utilized for the preparation of new metal oxides or carbon nanomaterials by thermal decomposition. In MOFs, the highly ordered metal ions are isolated by organic ligands regularly, which would play an important role in preventing metal aggregation during thermolysis. These MOF-derived materials have shown excellent performance in a variety of applications such as heterogeneous catalysis,[8] electrochemistry,[9] and gas adsorption.[10] To the best of our knowledge, so far reports on the use of such MOF-derived materials as catalysts for liquid-phase organic synthesis are rare.

ZIF-67 (Co(MeIM)$_2$, MeIM = 2-methylimidazole) was selected as the MOF precursor due to its good thermal stability, and high nitrogen and carbon content with zero oxygen content. The strong coordination interaction between Co and N atoms would allow a stepwise collapse of the MOF structure during the slow-heating procedures to prevent a serious aggregation of Co. The MeIM linkers will be carbonized gradually and the resulting carbon–nitrogen composite will play an important role in isolating the Co species (Figure 1).
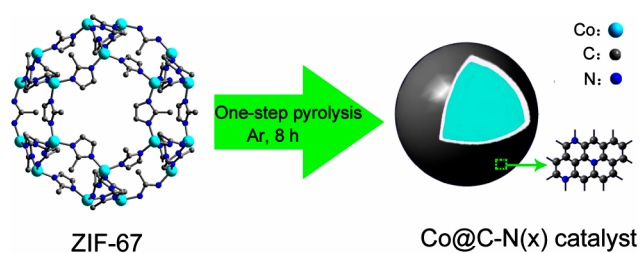

Figure 1. Schematic illustration of formation of a nitrogen doped graphite embedded Co catalyst from one-step pyrolysis of ZIF-67.

Since nitrogen doping can be an effective way to enhance the performance of carbon materials,[11] the nitrogen content remaining in the final material could be maximized due to the absence of oxygen atoms in the selected MOF.

■ RESULTS AND DISCUSSION

ZIF-67 was prepared from cobalt nitrate and 2-methylimidazole by a room-temperature precipitation method.[12] The powder X-ray diffraction (XRD) patterns of as-synthesized ZIF-67 (Figure S1 in the Supporting Information) matched well with the simulated and also the published XRD patterns, confirming the formation of pure ZIF-67 crystals.[13] The MOF material clearly showed the typical rhombic dodecahedral shape with particle sizes of around 300 nm, as can be seen from scanning electron microscopy (SEM) images (Figure S2a in the Supporting Information). The formation of MOF crystals with a smaller particle size in comparison to those prepared by using the general synthesis method (normally with a crystal size of submillimeters)[14] may be beneficial for the preparation of small Co@C-N particles and thereby for enhanced catalytic activity because of an improved active surface. The conversion of ZIF-

67 into Co@C-N materials was performed by direct thermal treatments under a flow of argon. As observed from the TGA-DSC curves (Figure S3 in the Supporting Information), ZIF-67 began to decompose when the temperature was increased to ca. 500 °C under argon. Therefore, four different target temperatures (i.e., 600, 700, 800, and 900 °C) were set with a heating rate of 1 °C/min from room temperature. The ZIF-67 crystals were annealed at the final temperatures for 8 h to produce the Co@C-N composites. The prepared material is denoted as Co@C-N(x), where x indicates the MOF pyrolysis temperature. SEM images (Figure S2) of Co@C-N(x) exhibited relatively smaller particles and increasingly rougher surface in comparison to the parent ZIF-67, indicating the gradual decomposition and carbonization of the frameworks. The Co contents in the Co@C-N(x) materials were about 30–40 wt % (Table S1 in the Supporting Information). The EDS element mapping revealed the uniform distributions of Co, C, and N elements in the Co@C-N materials (Figure S4 in the Supporting Information). Nitrogen adsorption isotherms at 77 K (Figure S5 in the Supporting Information) showed typically microporous structures of the Co@C-N(x) materials with specific surface areas of around 300–400 m^2 g^{-1} (Table S1).

The XRD patterns of the Co@C-N composites (Figure 2) showed five diffraction peaks at around 44.2, 51.6, 76.0, 92.4,
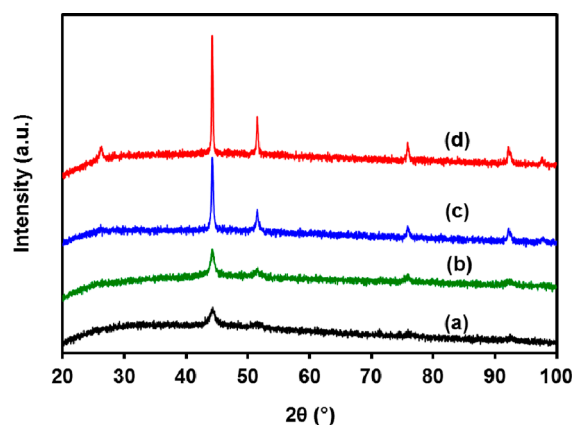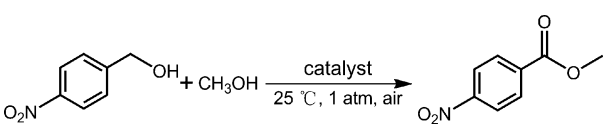

Figure 2. Powder XRD patterns of (a) Co@C-N(600), (b) Co@C-N(700), (c) Co@C-N(800), and (d) Co@C-N(900).

and 97.8°, respectively, characteristic of metallic Co (JCPDS No. 15-0806). The improved intensities of the Co diffraction peaks for the materials prepared at higher pyrolysis temperatures indicated the production of a Co phase with a higher crystallization degree. The XRD peak at ca. 25.8° observed clearly at relatively high temperatures corresponds to the interlayer d spacing of 3.42 Å, which can be assigned to the turbostratic ordering of the carbon and nitrogen atoms in the graphite layers.[15]

The catalytic activities of the prepared materials were tested using the oxidative cross esterification of p-nitrobenzyl alcohol and methanol as a model reaction. Reactions were performed at room temperature (25 °C) and atmospheric pressure using air as oxidant under base-free conditions. The results are summarized in Table 1. The parent ZIF-67 gave no conversion of p-nitrobenzyl alcohol, suggesting that cobalt ions coordinated with 2-methylimidazole were not active for alcohol oxidation under the investigated conditions (Table 1, entry 1). To our delight, ZIF-67 pyrolyzed materials were highly active in

Table 1. Oxidative Esterification of *p*-Nitrobenzyl Alcohol with Methanol[a]

entry	catalyst	conversion (%)	yield (%)[b]
1	ZIF-67		
2	Co@C-N(600)	76	74
3	Co@C-N(700)	89	88
4	Co@C-N(800)	>99	>99
5	Co@C-N(900)	55	52
6[c]	Co@C-N(800)	98	97
7[d]	Co@C-N(800)	72	61
8[e]	Co@C-N(800)	>99	>99
9[f]	Co@C-N(800)	>99	>99
10	Co@C-N(800)-H+		
11	Co@C-N(800)-air	5	4
12[g]	Co + C		

[a]Reaction conditions unless specified otherwise: *p*-nitrobenzyl alcohol (0.5 mmol), CH_3OH (1 mL), *n*-hexane (4 mL), catalyst (Co 15 mol %), *p* = 1 atm, 25 °C, in air, 96 h. [b]GC yield based on *p*-nitrobenzyl alcohol. [c]CH_3OH (2.5 mmol). [d]CH_3OH (0.5 mmol). [e]K_2CO_3 (0.1 mmol), 48 h. [f]60 °C, 20 h. [g]Physical mixture of commercial Co and carbon powder; the Co and C contents are the same as those of Co@C-N(800).

this transformation, and Co@C-N(800) exhibited the highest efficiency with respect to both conversion and selectivity (Figure S6 in the Supporting Information), affording the desired product methyl *p*-nitrobenzoate in >99% yield (Table 1, entries 2−5). Such a high reactivity and selectivity in the oxidative esterification of alcohols at room temperature under atmospheric conditions in the absence of base additives by using non-noble metals as catalyst has not been reported to date. When the thermolysis temperature was further increased to 900 °C, the reactivity of the resulting material decreased significantly (Table 1, entry 5). *p*-Nitrobenzaldehyde was detected as the main byproduct, especially at lower conversions (Figure S6), which is consistent with a two-step mechanism involving the first oxidation of alcohol to aldehyde and further reaction with alcohol to produce the ester.[5a] In addition, the latter reaction might be the rate-determining step in the direct oxidative esterification of alcohols. It is noteworthy that the reaction could also proceed at lower methanol loadings (even stoichiometrically), albeit less efficiently (Table 1, entries 6 and 7). As expected, the addition of base remarkably accelerated the reaction and shortened the time needed to complete the conversion (Table 1, entry 8).

Although Co_3O_4 nanoparticles from the direct thermolysis of MOFs have been described as high-performance materials for supercapacitors,[16] lithium ion batteries,[17] catalytic oxidation of CO,[18] gas sensing,[19] and gas adsorption,[20] thus far, reports on the use of such MOF-derived Co materials for liquid-phase catalytic reactions are rare. In this regard, the recent work by Beller and co-workers is noteworthy, which reports a novel Co_3O_4-N@C material by pyrolysis of nitrogen-ligated cobalt-(II) acetate supported on commercial carbon for the direct oxidative esterification of alcohols.[21] Good to excellent yields were achieved using pure oxygen as oxidant at 60−120 °C in the presence of catalytic amounts of K_2CO_3 as base over the Co_3O_4-N@C catalyst. For example, the reaction of *p*-nitro-

benzyl alcohol and methanol gave an 88% yield within 24 h at 60 °C.[21] Under identical conditions, the present Co@C-N(800) catalyst furnished a quantitative yield of methyl *p*-nitrobenzoate in 8 h. Note in the present study that although the time to complete conversion of *p*-nitrobenzyl alcohol was a little long (i.e., 96 h) at 25 °C in air in the absence of basic promoters, it could be significantly shortened at slightly higher temperatures: e.g., within 20 h at 60 °C over the Co@C-N(800) catalyst (Table 1, entry 9).

The recyclability of the catalyst was investigated because it is crucial that a highly active catalyst may be reused. After the reaction with Co@C-N(800), a magnet was placed close to the reactor wall. Very quickly, all the powders were adsorbed on the wall by the magnet (Figure S7 in the Supporting Information), implying the good magnetic properties of the Co-based material. Thus, the catalyst could be easily separated from the reaction mixture just by pouring the solution. The remainng solids were washed with methanol and then reused as the catalyst under identical reaction conditions. The oxidative esterfication result over the reused catalyst showed that the activity significantly decreased. However, to our delight, the reactivity could be fully restored when the reused catalyst was treated in H_2 at 400 °C for 1 h, and no apparent loss in efficiency was observed for up to five runs (Figure S8 in the Supporting Information). PXRD results (Figure S9 in the Supporting Information) indicated that the Co diffraction peaks of the reused catalyst without H_2 treatment were much weaker than those of the fresh catalyst, suggesting that the metallic Co was probably partially oxidized during the course of the reaction by oxygen in air. After reduction, it was observed that the strengths of the Co diffraction peaks increased to the same levels as those for the fresh catalyst. This result could account for the recovery of the catalytic activity of Co@C-N(800) upon reduction treatment.

A leaching experiment was performed to further check the stability of the Co nanoparticles and to verify the heterogeneous nature of the reaction. The reaction with the solution after filtration at approximately 35% conversion essentially stopped, strongly suggesting that the reaction was predominantly heterogeneous (Figure S10 in the Supporting Information). Moreover, Co@C-N(800) showed negligible cobalt leaching during the reaction. We considered that the Co nanoparticles were well embedded in the C−N composite (see TEM images as shown below), and thus the cobalt leaching could be efficiently prohibited. These results demonstrated that the highly active Co@C-N(800) catalyst was stable and reusable under mild reaction conditions.

To identify the active sites for aerobic oxidative esterification of alcohols, we examined the catalytic efficiency of Co@C-N(800) after removing the metallic Co or C-N composite under identical conditions. First, the as-synthesized Co@C-N(800) was immersed in aqua regia to completely remove Co (Table S1 and Figure S11 in the Supporting Information), and the resulting material is denoted as Co@C-N(800)-H+. Co@C-N(800)-H+ was not active in the oxidation of alcohols, demonstrating the requirement of a metal to catalyze the reaction (Table 1, entry 10). On the other hand, the Co@C-N(800) material was subjected to heating at 400 °C for 0.5 h in air and then for 1 h under hydrogen. The C−N composite was mostly burned (Table S1 and Figure S11) after this heating treatment, and the resulting material is denoted as Co@C-N(800)-air. The XRD of Co@C-N(800)-air exhibited a mixture of face-centered cubic (fcc) and hexagonally close

packed (hcp) cobalt, which is often observed for Co after treatment at high temperatures.[22] Co@C-N(800)-air showed little activity and produced methyl *p*-nitrobenzoate in only 4% yield (Table 1, entry 11). Interestingly, a physical mixture of commercial metallic cobalt (20−30 nm) and activated carbon also showed no reactivity (Table 1, entry 12). These control experiments suggest the important synergic interactions between C−N composite and Co in determining the activity of Co@C-N(800) in the oxidative esterification.

To elucidate reasons for the remarkable catalytic activity of the Co@C-N(800) material, the effects of pyrolysis temperature on the structures of the catalysts were studied in detail by high-resolution transmission electron microscopy (HRTEM) and X-ray photoelectron spectroscopy (XPS). No significant aggregation of Co nanoparticles was observed for Co@C-N pyrolyzed at even a temperature as high as 800 °C (Figure 3
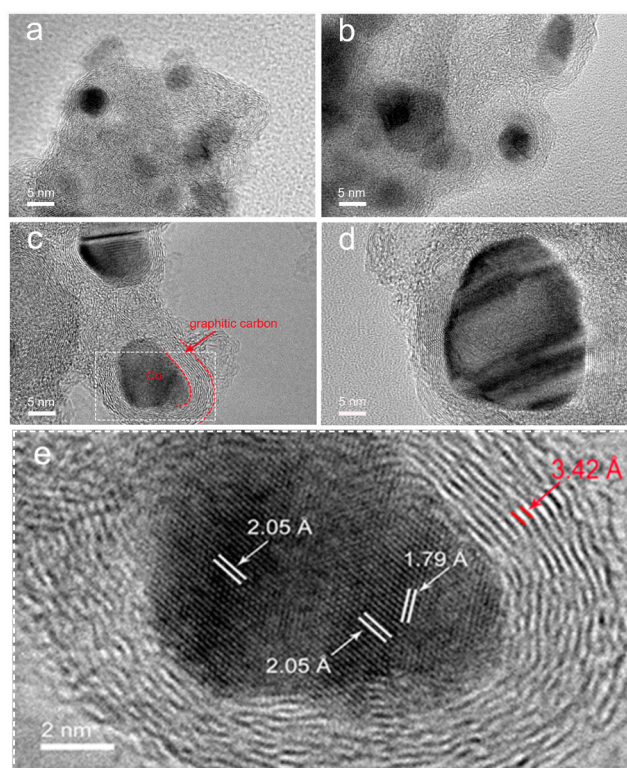
Figure 3. HRTEM images of (a) Co@C-N(600), (b) Co@C-N(700), (c) Co@C-N(800), and (d) Co@C-N(900). The red lines in (c) indicate a Co nanoparticle wrapped by graphite layers. Panel (e) shows an enlarged image of a Co particle in (c).

and Figure S12 in the Supporting Information), which could be attributed to the separation effect of carbons formed from carbonization of the 2-methylimidazole linker in ZIF-67. The size of Co crystals was in good agreement with that estimated from XRD for each sample. Each Co nanoparticle in Co@C-N(800) was surrounded tightly by graphitized carbon. This phenomenon is consistent with the literature works that have reported on the use of transition metals for the catalytic graphitization of carbon.[23] The graphite-enclosed Co nanoparticles in Co@C-N(800) were highly crystallized (Figure 3e) and exhibited two fringe spacings of 2.05 and 1.79 Å, corresponding to the (111) and (200) planes in fcc cobalt, respectively.[24] In addition to structures similar to that of Co@C-N(800), we observed the formation of a large number of

carbon nanotubes when the pyrolysis temperature was increased to 900 °C (Figure S12d), as was also evident in the SEM images (Figure S2e in the Supporting Information). The presence of Co nanoparticles at the tip of the tubes suggests that the growth of carbon nanotubes was catalyzed by the generated Co nanoparticles. As seen from the TEM images, the growth of tubes resulted in serious aggregation of Co nanoparticles, which may be the crucial reason for the low catalytic activity of Co@C-N(900) in the oxidative esterification reaction.

To gain further insight into the catalyst structure and especially the location of nitrogen, XPS characterization was performed on the samples. In the cobalt region, only peaks characteristic of metallic Co were observed (Figure S13 in the Supporting Information) with the typical binding energies of 793.6 and 778.8 eV, assigned to Co $2p_{1/2}$ and Co $2p_{3/2}$ electrons of Co metal, respectively. In the parent ZIF-67, one N 1s peak occurred at 398.7 eV (Figure 4), which is related to
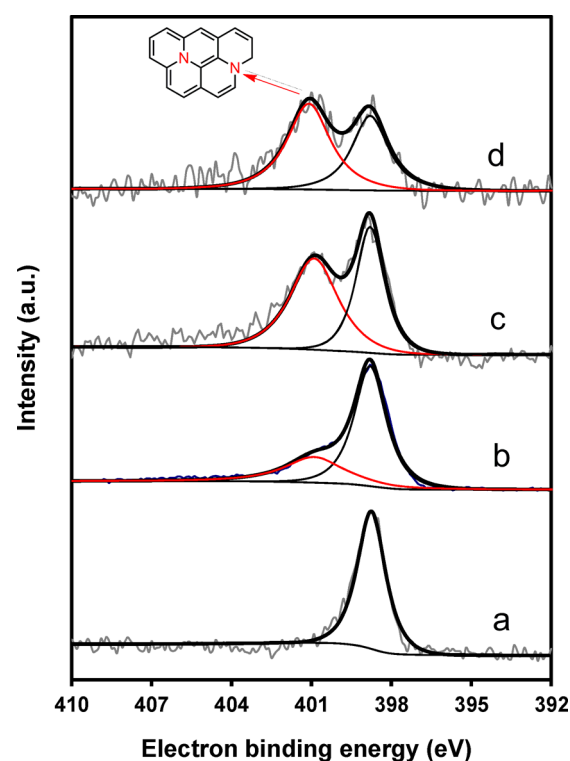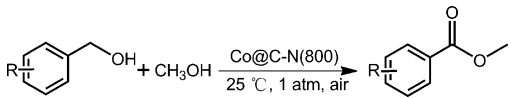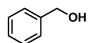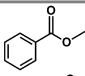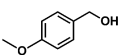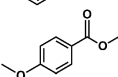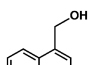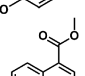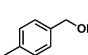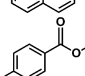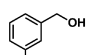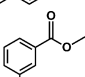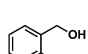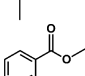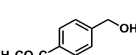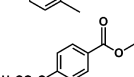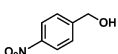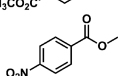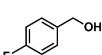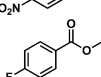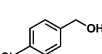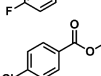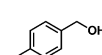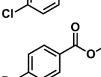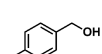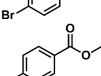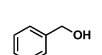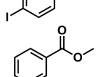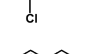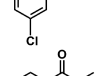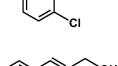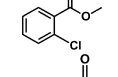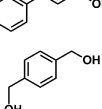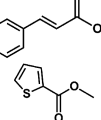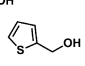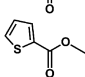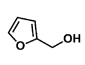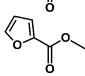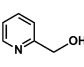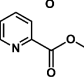

Figure 4. N 1s spectra for (a) ZIF-67, (b) Co@C-N(700), (c) Co@C-N(800), and (d) Co@C-N(900).

pyridinic nitrogen coordinating to a cobalt ion.[25] A new N 1s peak at 401.0−402.0 eV was observed in the Co@C-N materials, which may be assigned to nitrogen in a graphitic structure.[26] Moreover, the ratio of graphitic nitrogen to pyridinic nitrogen in Co@C-N was increased when the pyrolysis temperature was enhanced (e.g., 0.4 for 700 °C, 1.2 for 800 °C, and 1.4 for 900 °C), implying a higher graphitization degree at higher temperatures. This result is in good agreement with the TEM and XRD observations.

The scope of the presented methodology was then extended to the oxidative esterification of a series of structurally diverse aromatic alcohols under similar reaction conditions using the Co@C-N(800) catalyst. As can be seen from Table 2, various benzylic alcohols were selectively converted into the corresponding methyl esters in excellent yields at room temperature

Table 2. Oxidative Esterification of Aromatic Alcohols with Methanol[a]

Entry	Alcohol	Product	Yield (%)[b]
1			>99
2			>99
3			>99
4			>99
5			94
6[c]			86
7			>99
8			>99
9			98
10			>99
11			>99
12			>99
13			94
14			90
15			>99
16			>99
17[d]			80
18[d]			88
19[d]			93

[a]Reaction conditions unless specified otherwise: aromatic alcohol (0.5 mmol), CH$_3$OH (1 mL), n-hexane (4 mL), Co@C-N(800) (Co 15 mol %), p = 1 atm, in air, 25 °C, 96 h. [b]GC yield based on benzylic alcohol. Aromatic aldehydes were the main byproducts. [c]Conditions same as in footnote a at 108 h. [d]Conditions same as in footnote a with 25 mol % Co at 120 h.
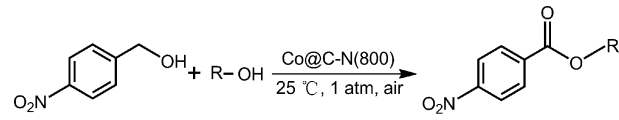
under atmospheric conditions without the addition of any base additives. The desired esters were obtained in >99% yields
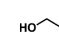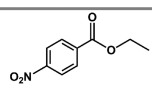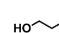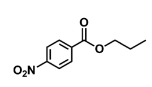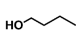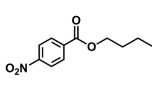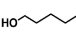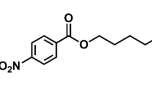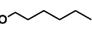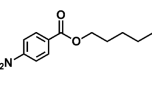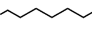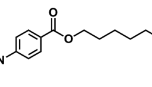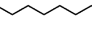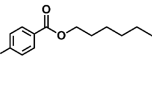
when benzylic alcohols substituted with strongly electron-donating groups such as p-OMe were employed (Table 2, entries 2 and 3). The different substituted positions on the phenyl ring had a marked influence on the reactivity of the reaction. As an example, the methyl group at meta and ortho positions showed a lower activity to the desired ester in comparison with that in the para position (Table 2, entries 4–6). Apart from electron-donating groups, benzylic alcohols substituted with various electron-withdrawing groups, such as −CO$_2$CH$_3$, −NO$_2$, −F, −-Cl, −Br, and −I, all reacted with methanol smoothly, giving the desired esters in >90% yields (Table 2, entries 7–14). Notably, even more sensitive allylic alcohols such as cinnamic alcohol underwent the oxidative esterification in quantitative yield (Table 2, entry 15). Furthermore, a diol could be completely converted into the corresponding diester in >99% yield (Table 2, entry 16).

It is worth noting that heterocycles such as thiophene-2-methanol, furan-2-methanol, and pyridine-2-methanol could also be used as substrates in the oxidative esterification reaction and afforded the heterocyclic carboxylic acid esters in up to 93% yield (Table 2, entries 17–19).

After successful application of the cross esterification to methanol with various benzylic alcohols, we tried to extend this novel catalytic system to the oxidative esterification of long-chain aliphatic alcohols. Various linear aliphatic alcohols including ethyl, n-propyl, n-but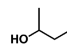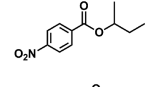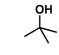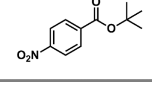yl, n-pentyl, n-hexyl, n-heptyl, and even n-octyl alcohol underwent the esterification smoothly to furnish the corresponding esters in good to excellent yields at room temperature under atmospheric and base-free conditions (Table 3, entries 1–7). A gradual decrease in product yield was observed when the carbon chain length of the aliphatic alcohol increased. However, a high yield of the desired product could still be achieved simply by prolonging the reaction time: e.g., for the oxidative esterification of n-octyl alcohol (Table 3, entry 7). The present catalytic system is also applicable to the oxidative esterification of branched alcohols. Not surprisingly, such cross esterifications are difficult to achieve in high yield and have been rarely investigated in the literature due to the possible oxidation of one alcohol in the presence of another. The desired ester was obtained in 81% yield when isobutyl alcohol was employed (Table 3, entry 8). The yield to the cross esterification product decreased remarkably as the steric hindrance of alcohol increased: e.g., for tert-butyl alcohol, the desired product was obtained in 62% yield under identical conditions (Table 3, entry 9).

The application of the newly developed oxidative esterification protocol was further extended to the lactonization of diols. Lactones are ubiquitous as structural elements in various bioactive natural products and synthetic organic compounds. The oxidative lactonization of diols using molecular oxygen as oxidant is an attractive methodology for the synthesis of lactones. Nevertheless, so far the developed catalytic protocols were usually based on homogeneous catalysts or noble metals such as Au, Ru, Pd, and Ir.[27] Here, 1,2-benzenedimethanol was the first diol used in the oxidative lactonization reaction over the Co@C-N(800) catalyst. The desired lactone was obtained in 97% yield at room temperature and atmospheric conditions without the assistance of any base additives (Table 4, entry 1). The catalyst system was also applicable to the oxidative lactonization of aliphatic α,ω-diols ranging from 1,4- to 1,8-diols, affording the corresponding lactones in excellent yields under mild reaction conditions (Table 4, entries 2–6). It is noteworthy that there have only been a few reports to date on

Table 3. Oxidative Esterification of *p*-Nitrobenzyl Alcohol with Various Aliphatic Alcohols[a]

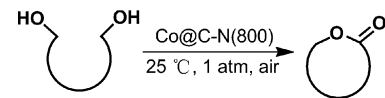| Entry	Aliphatic alcohol	Product	Yield (%)[b]
1			99
2			97
3			95
4			91
5			86
6			80
7[c]			82
8			81
9			62

[a]Reaction conditions unless specified otherwise: *p*-nitrobenzyl alcohol (0.5 mmol), aliphatic alcohol (2 mL), *n*-hexane (3 mL), Co@C-N(800) (Co 40 mol %), p = 1 atm, in air, 25 °C, 96 h. Aldehydes and esters from aliphatic alcohols (e.g., ethyl acetate) were observed. [b]GC yield based on benzylic alcohol. [c]Conditions same as those in footnote *a* at 120 h.
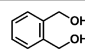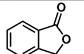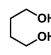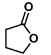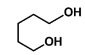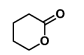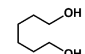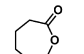
the catalytic synthesis of lactones with large-membered rings from lactonization of diols.[28] The reaction results of different alcohols (Tables 2−4) demonstrate the general applicability of the novel catalyst system in selective oxidative esterification.

In a final set of experiments, we examined the synthetic utility of our catalyst system under scale-up conditions. We performed 10 mmol scale reactions for selected substrates, and the results are shown in Table S2 in the Supporting Information. It can be seen that all of these substrates underwent the oxidative esterification smoothly, furnishing the corresponding esters in 95−97% isolated yields under scale-up conditions. These results verified that the proposed protocol for ester synthesis from the oxidation of alcohols is scalable under the investigated conditions.

CONCLUSIONS

In summary, we have developed a general, simple, cost-effective, and environmentally friendly protocol for direct aerobic oxidative esterification of alcohols, using a novel nitrogen doped graphite enclosed cobalt material as catalyst.

Table 4. Lactonization of Various Diols[a]

Entry	Diol	Product	Yield (%)[b]
1			97
2			96
3			93
4			92
5			90
6			90

[a]Reaction conditions: diol (0.5 mmol), *n*-hexane (5 mL), Co@C-N(800) (Co 40 mol %), p = 1 atm, in air, 25 °C, 96 h. [b]GC yield based on diol. Inner ethers were detected as the main byproducts.

The catalyst is prepared by one-pot thermolysis of a Co-based MOF with high nitrogen and carbon contents. The catalytic system features a broad substrate scope for aromatic and aliphatic alcohols as well as diols, giving their corresponding esters in good to excellent yields at room temperature and atmospheric conditions without the assistance of any base additives. The initial success in achieving select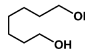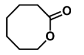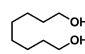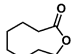ive oxidative esterification of alcohols using MOF-pyrolyzed materials might provide a new avenue for developing new types of composite materials for highly efficient catalytic organic transformations.

■ ASSOCIATED CONTENT

Ⓢ Supporting Information
The following file is available free of charge on the ACS Publications website at DOI: 10.1021/cs502101c.

   Experimental details, characterization data, and spectra of products (PDF)

■ AUTHOR INFORMATION

Corresponding Author
*E-mail for Y.L.: liyw@scut.edu.cn.

Notes
The authors declare no competing financial interest.

■ ACKNOWLEDGMENTS

■ REFERENCES

(1) Otera, J.; Nishikido, J. *Esterification: methods, reactions, and applications*; Wiley: Hoboken, NJ, 2009; p 1.

(2) (a) Otera, J. *Chem. Rev.* **1993**, *93*, 1449−1470. (b) Larock, R. C. *Comprehensive organic transformations: a guide to functional group preparations*; Wiley-VCH: New York, 1999; Vol. *1*, pp 1−2640. (c) Chau, K. D.; Duus, F.; Le, T. N. *Green Chem. Lett. Rev.* **2013**, *6*, 89−93. (d) Nguyen, J. D.; D'Amato, E. M.; Narayanam, J. M.; Stephenson, C. R. *Nat. Chem.* **2012**, *4*, 854−859.

(3) (a) Gopinath, R.; Barkakaty, B.; Talukdar, B.; Patel, B. K. *J. Org. Chem.* **2003**, *68*, 2944−2947. (b) Gopinath, R.; Patel, B. K. *Org. Lett.* **2000**, *2*, 577−579. (c) Malik, P.; Chakraborty, D. *Tetrahedron Lett.* **2010**, *51*, 3521−3523. (d) Suzuki, K.; Yamaguchi, T.; Matsushita, K.; Iitsuka, C.; Miura, J.; Akaogi, T.; Ishida, H. *ACS Catal.* **2013**, *3*, 1845−1849. (e) Delany, E. G.; Fagan, C. L.; Gundala, S.; Mari, A.; Broja, T.; Zeitler, K.; Connon, S. J. *Chem. Commun.* **2013**, *49*, 6510−6512. (f) Delany, E. G.; Fagan, C.-L.; Gundala, S.; Zeitler, K.; Connon, S. J. *Chem. Commun.* **2013**, *49*, 6513−6515. (g) Rafiee, E.; Eavani, S. *J. Mol. Catal. A-Chem.* **2013**, *373*, 30−37.

(4) (a) Liu, C.; Wang, J.; Meng, L.; Deng, Y.; Li, Y.; Lei, A. *Angew. Chem., Int. Ed.* **2011**, *50*, 5144−5148. (b) Miyamura, H.; Yasukawa, T.; Kobayashi, S. *Green Chem.* **2010**, *12*, 776−778. (c) Oliveira, R. L.; Kiyohara, P. K.; Rossi, L. M. *Green Chem.* **2009**, *11*, 1366−1370. (d) Marsden, C.; Taarning, E.; Hansen, D.; Johansen, L.; Klitgaard, S. K.; Egeblad, K.; Christensen, C. H. *Green Chem.* **2008**, *10*, 168−170. (e) Su, F. Z.; Ni, J.; Sun, H.; Cao, Y.; He, H. Y.; Fan, K. N. *Chem. Eur. J.* **2008**, *14*, 7131−7135. (f) Yamamoto, N.; Obora, Y.; Ishii, Y. *J. Org. Chem.* **2011**, *76*, 2937−2941. (g) Wang, H.; Li, L.; Bai, X. F.; Shang, J. Y.; Yang, K. F.; Xu, L. W. *Adv. Synth. Catal.* **2013**, *355*, 341−347. (h) Gowrisankar, S.; Neumann, H.; Beller, M. *Angew. Chem., Int. Ed.* **2011**, *50*, 5139−5143.

(5) (a) Kaizuka, K.; Miyamura, H.; Kobayashi, S. *J. Am. Chem. Soc.* **2010**, *132*, 15096−15098. (b) Parreira, L. A.; Bogdanchikova, N.; Pestryakov, A.; Zepeda, T. A.; Tuzovskaya, I.; Farías, M. H.; Gusevskaya, E. V. *Appl. Catal. A: Gen.* **2011**, *397*, 145−152. (c) Kegnæs, S.; Mielby, J.; Mentzel, U. V.; Jensen, T.; Fristrup, P.; Riisager, A. *Chem. Commun.* **2012**, *48*, 2427−2429. (d) Hao, Y.; Chong, Y.; Li, S.; Yang, H. *J. Phys. Chem. C* **2012**, *116*, 6512−6519. (e) Asao, N.; Hatakeyama, N.; Minato, T.; Ito, E.; Hara, M.; Kim, Y.; Yamamoto, Y.; Chen, M. W.; Zhang, W.; Inoue, A. *Chem. Commun.* **2012**, *48*, 4540−4542. (f) Costa, V. V.; Estrada, M.; Demidova, Y.; Prosvirin, I.; Kriventsov, V.; Cotta, R. F.; Fuentes, S.; Simakov, A.; Gusevskaya, E. V. *J. Catal.* **2012**, *292*, 148−156. (g) Liu, P.; Li, C.; Hensen, E. J. *Chem. Eur. J.* **2012**, *18*, 12122−12129.

(6) Powell, A. B.; Stahl, S. S. *Org. Lett.* **2013**, *15*, 5072−5075.

(7) (a) Furukawa, H.; Cordova, K. E.; O'Keeffe, M.; Yaghi, O. M. *Science* **2013**, *341*, 1230444. (b) Corma, A.; Garcia, H.; Llabrés i Xamena, F. X. *Chem. Rev.* **2010**, *110*, 4606−4655. (c) Yuan, B. Z.; Pan, Y. Y.; Li, Y. W.; Yin, B. L.; Jiang, H. F. *Angew. Chem., Int. Ed.* **2010**, *49*, 4054−4058. (d) Murray, L. J.; Dincă, M.; Long, J. R. *Chem. Soc. Rev.* **2009**, *38*, 1294−1314. (e) Lee, J.; Farha, O. K.; Roberts, J.; Scheidt, K. A.; Nguyen, S. T.; Hupp, J. T. *Chem. Soc. Rev.* **2009**, *38*, 1450−1459. (f) Sun, C. Y.; Wang, X. L.; Zhang, X.; Qin, C.; Li, P.; Su, Z. M.; Zhu, D. X.; Shan, G. G.; Shao, K. Z.; Wu, H.; Li, J. *Nat. Commun.* **2013**, *4*, 2717−2725. (g) Farha, O. K.; Yazaydin, A. O.; Eryazici, I.; Malliakas, C. D.; Hauser, B. G.; Kanatzidis, M. G.; Nguyen, S. T.; Snurr, R. Q.; Hupp, J. T. *Nat. Chem.* **2010**, *2*, 944−948.

(8) (a) Zhao, H.; Song, H.; Xu, L.; Chou, L. *Appl. Catal. A: Gen.* **2013**, *456*, 188−196. (b) Zhang, F.; Chen, C.; Xiao, W.-m.; Xu, L.; Zhang, N. *Catal. Commun.* **2012**, *26*, 25−29. (c) Yang, Y.; Jia, L.; Hou, B.; Li, D.; Wang, J.; Sun, Y. *J. Phys. Chem. C* **2014**, *118*, 268−277.

(9) (a) Yang, S. J.; Nam, S.; Kim, T.; Im, J. H.; Jung, H.; Kang, J. H.; Park, C. R. *J. Am. Chem. Soc.* **2013**, *135*, 7394−7397. (b) Amali, A. J.; Sun, J.-K.; Xu, Q. *Chem. Commun.* **2014**, *50*, 1519−1522. (c) Chaikittisilp, W.; Torad, N. L.; Li, C.; Imura, M.; Suzuki, N.; Ishihara, S.; Yamauchi, Y. *Chem. Eur. J.* **2014**, *20*, 4217−4221.

(10) (a) Kim, T. K.; Lee, K. J.; Cheon, J. Y.; Lee, J. H.; Joo, S. H.; Moon, H. R. *J. Am. Chem. Soc.* **2013**, *135*, 8940−8946. (b) Jiang, H. L.; Liu, B.; Lan, Y. Q.; Kuratani, K.; Akita, T.; Shioyama, H.; Xu, Q. *J. Am. Chem. Soc.* **2011**, *133*, 11854−11857. (c) Srinivas, G.; Krungleviciute, V.; Guo, Z. X.; Yildirim, T. *Energy Environ. Sci.* **2014**, *7*, 335−342. (d) Almasoudi, A.; Mokaya, R. *J. Mater. Chem.* **2012**, *22*, 146−152.

(11) (a) Zhong, M.; Kim, E. K.; McGann, J. P.; Chun, S. E.; Whitacre, J. F.; Jaroniec, M.; Kowalewski, T. *J. Am. Chem. Soc.* **2012**, *134*, 14846−14857. (b) Li, X. H.; Antonietti, M. *Chem. Soc. Rev.* **2013**, *42*, 6593−6604.

(12) Qian, J.; Sun, F.; Qin, L. *Mater. Lett.* **2012**, *82*, 220−223.

(13) Banerjee, R.; Phan, A.; Wang, B.; Knobler, C.; Furukawa, H.; O'Keeffe, M.; Yaghi, O. M. *Science* **2008**, *319*, 939−943.

(14) Saracco, G.; Vankova, S.; Pagliano, C.; Bonelli, B.; Garrone, E. *Phys. Chem. Chem. Phys.* **2014**, *16*, 6139−6145.

(15) Yang, Y.; Jia, L.; Hou, B.; Li, D.; Wang, J.; Sun, Y. *J. Phys. Chem. C* **2014**, *118*, 268−277.

(16) Meng, F.; Fang, Z.; Li, Z.; Xu, W.; Wang, M.; Liu, Y.; Guo, X. *J. Mater. Chem. A* **2013**, *1*, 7235−7241.

(17) Liu, B.; Zhang, X.; Shioyama, H.; Mukai, T.; Sakai, T.; Xu, Q. *J. Power Sources* **2010**, *195*, 857−861.

(18) Wang, W.; Li, Y.; Zhang, R.; He, D.; Liu, H.; Liao, S. *Catal. Commun.* **2011**, *12*, 875−879.

(19) Lü, Y.; Zhan, W.; He, Y.; Wang, Y.; Kong, X.; Kuang, Q.; Zheng, L. *ACS Appl. Mater. Interfaces* **2014**, *6*, 4186−4195.

(20) Das, R.; Pachfule, P.; Banerjee, R.; Poddar, P. *Nanoscale* **2012**, *4*, 591−599.

(21) Jagadeesh, R. V.; Junge, H.; Pohl, M. M.; Radnik, J.; Brückner, A.; Beller, M. *J. Am. Chem. Soc.* **2013**, *135*, 10776−10782.

(22) Puntes, V. F.; Krishnan, K. M.; Alivisatos, A. P. *Science* **2001**, *291*, 2115−2117.

(23) (a) Fu, R.; Baumann, T. F.; Cronin, S.; Dresselhaus, G.; Dresselhaus, M. S.; Satcher, J. H. *Langmuir* **2005**, *21*, 2647−2651. (b) Maldonado-Hodar, F. J.; Moreno-Castilla, C.; Rivera-Utrilla, J.; Hanzawa, Y.; Yamada, Y. *Langmuir* **2000**, *16*, 4367−4373.

(24) Nam, K. M.; Shim, J. H.; Ki, H.; Choi, S. I.; Lee, G.; Jang, J. K.; Park, J. T. *Angew. Chem., Int. Ed.* **2008**, *47*, 9504−9508.

(25) Westerhaus, F. A.; Jagadeesh, R. V.; Wienhöfer, G.; Pohl, M. M.; Radnik, J.; Surkus, A. E.; Beller, M. *Nat. Chem.* **2013**, *5*, 537−543.

(26) Jaouen, F.; Herranz, J.; Lefevre, M.; Dodelet, J. P.; Kramm, U. I.; Herrmann, I.; Ustinov, E. A. *ACS Appl. Mater. Interfaces* **2009**, *1*, 1623−1639.

(27) (a) Li, X.; Cui, Y.; Yang, X.; Dai, W. L.; Fan, K. *Appl. Catal. A: Gen.* **2013**, *458*, 63−70. (b) Musa, S.; Shaposhnikov, I.; Cohen, S.; Gelman, D. *Angew. Chem., Int. Ed.* **2011**, *50*, 3533−3537. (c) Kwon, M. S.; Kim, N.; Park, C. M.; Lee, J. S.; Kang, K. Y.; Park, J. *Org. Lett.* **2005**, *7*, 1077−1079.

(28) (a) Endo, Y.; Bäckvall, J. E. *Chem. Eur. J.* **2011**, *17*, 12596−12601. (b) Jung, H. M.; Choi, J. H.; Lee, S. O.; Kim, Y. H.; Park, J. H.; Park, J. *Organometallics* **2002**, *21*, 5674−5677. (c) Suzuki, T.; Morita, K.; Tsuchida, M.; Hiroi, K. *Org. Lett.* **2002**, *4*, 2361−2363.